Journal of Biomolecular NMR, 2 (1992) 211–226
ESCOM

J-Bio NMR 060

Application of 2D and 3D NMR experiments to the conformational study of a diantennary oligosaccharide

P. de Waard[a], B.R. Leeflang[a], J.F.G. Vliegenthart[a], R. Boelens[b], G.W. Vuister[b] and R. Kaptein[b,*]

[a]*Bijvoet Center, Department of Bio-Organic Chemistry, Utrecht University, Padualaan 8, 3584 CH Utrecht, The Netherlands*
[b]*Bijvoet Center, Department of NMR Spectroscopy, Utrecht University, Padualaan 8, 3584 CH Utrecht, The Netherlands*

Received 19 July 1991
Accepted 8 January 1992

Keywords: Conformational analysis; Multidimensional NMR; Oligosaccharides

SUMMARY

By the application of homonuclear 3D NOE-HOHAHA and heteronuclear 3D HMQC-NOE experiments in studies of complex oligosaccharides, NOEs can be investigated which are hidden in conventional 2D NOE spectra. In the 3D NOE-HOHAHA spectrum ω_3 cross sections were considered to be the most suitable for assignment of NOEs. Alternatively, these cross sections could be measured separately in selective 2D HOHAHA-NOE spectroscopy. The advantages and limitations of the 2D alternative are compared with those of the 3D NOE-HOHAHA approach. In 3D HMQC-NOE spectroscopy the larger chemical shift displacement of the carbon spectrum with respect to the proton spectrum can be used to unmask NOEs hidden in the bulk region. If the extra proton dimension is not needed, 2D HMQC-NOE is a good alternative.

The suitability of 2D and 3D NOE-HOHAHA and HMQC-NOE experiments for the estimation of proton-proton distances is demonstrated by comparing the results of these experiments on a diantennary asparagine-linked oligosaccharide with those of a conventional 2D NOE experiment. NOEs identified in the 2D and 3D NOE-HOHAHA as well as HMQC-NOE experiments, so far not identified or not quantified in 2D NOE experiments, are discussed in relation to each glycosidic linkage. The flexibility of the Manα(1-3)Man linkage is demonstrated, confirming the existence of an ensemble of conformations for this linkage.

INTRODUCTION

High-resolution ^{1}H NMR spectroscopy has proven to be a powerful method in the structure elucidation of carbohydrates (Vliegenthart et al., 1983; Bush, 1989; Dabrowski, 1989; Homans, 1990). Structural information can be derived from parameters, such as chemical shifts, coupling constants, and relaxation rates. Average distances between protons can be calculated from

* To whom correspondence should be addressed.

through-space dipolar interactions, measured as NOEs. A major problem in the analysis of ^{1}H NMR spectra of carbohydrates is the overlap of resonances in the bulk region between 3 and 4 ppm. For this reason not every observable NOE can be identified in a conventional 2D NOE spectrum. With the aid of 3D NMR and/or the use of other NMR-sensitive nuclei many of these NOEs can be assigned, quantified and interpreted.

Torsion angles of the glycosidic linkages are important parameters defining the conformation of carbohydrates. The results from NOE experiments suggest that these torsion angles are restricted to narrow ranges of values. However, potential energy calculations demonstrated a shallow energy surface for glycosidic linkages (Cumming and Carver, 1987a,b). As a result, the lowest energy conformation may represent only a small part of the ensemble of relevant conformations (Carver et al., 1989). Since NOEs build up over hundreds of milliseconds, they correspond to an average of the ensemble of conformations. Therefore, a three-dimensional structure derived from a set of NOEs may represent a virtual conformation, which is not necessarily identical to the lowest energy conformation. An approach to this problem is to calculate the NOE intensities from the ensemble of conformations derived from potential energy functions (Cumming and Carver, 1987a).

In this report we explore new developments in NMR spectroscopy to investigate NOEs, so far not accessible for conformational studies. The results of homonuclear 3D NOE-HOHAHA (Vuister et al., 1989) and heteronuclear 3D HMQC-NOE (De Waard et al., 1990) experiments on the diantennary asparagine-linked oligosaccharide **1** are presented, as well as the 2D analogues of these experiments. 2D HMQC-NOE experiments were also performed on oligosaccharide **2**.

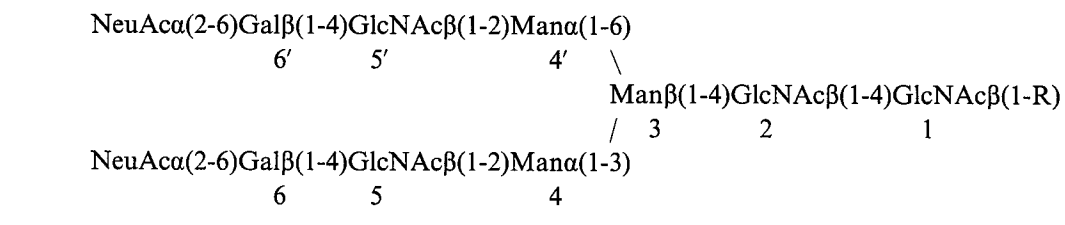

1: R = Asn; **2**: R = OH (α/β).

COMPARISON OF NMR METHODS

Homonuclear ^{1}H 2D and 3D experiments

Structural studies on oligosaccharides by means of ^{1}H NMR spectroscopy comprise the assignment of resonances and the analysis of NOE cross peaks. To a large extent this can be accomplished with 2D HOHAHA and 2D NOESY spectroscopy. To extract information which is hidden in these spectra because of overlap, both methods were combined in the form of 3D NOE-HOHAHA spectroscopy (Vuister et al., 1989). The pulse sequence for this experiment is shown in Fig. 1. For the spectral interpretation it is possible to use the isotropic mixing to assign protons hidden in the bulk region, followed by assignment of the NOEs of these protons. The data are presented in cross-sectional planes perpendicular to the ω_3 axis, called ω_3 cross sections (Vuister et al., 1989). As an example, a cross-sectional plane at the ω_3 frequency of the GlcNAc-1 H-1 at δ = 5.05 ppm of **1** is depicted in Fig. 2. The subspectrum of the GlcNAc-1 residue is found on the

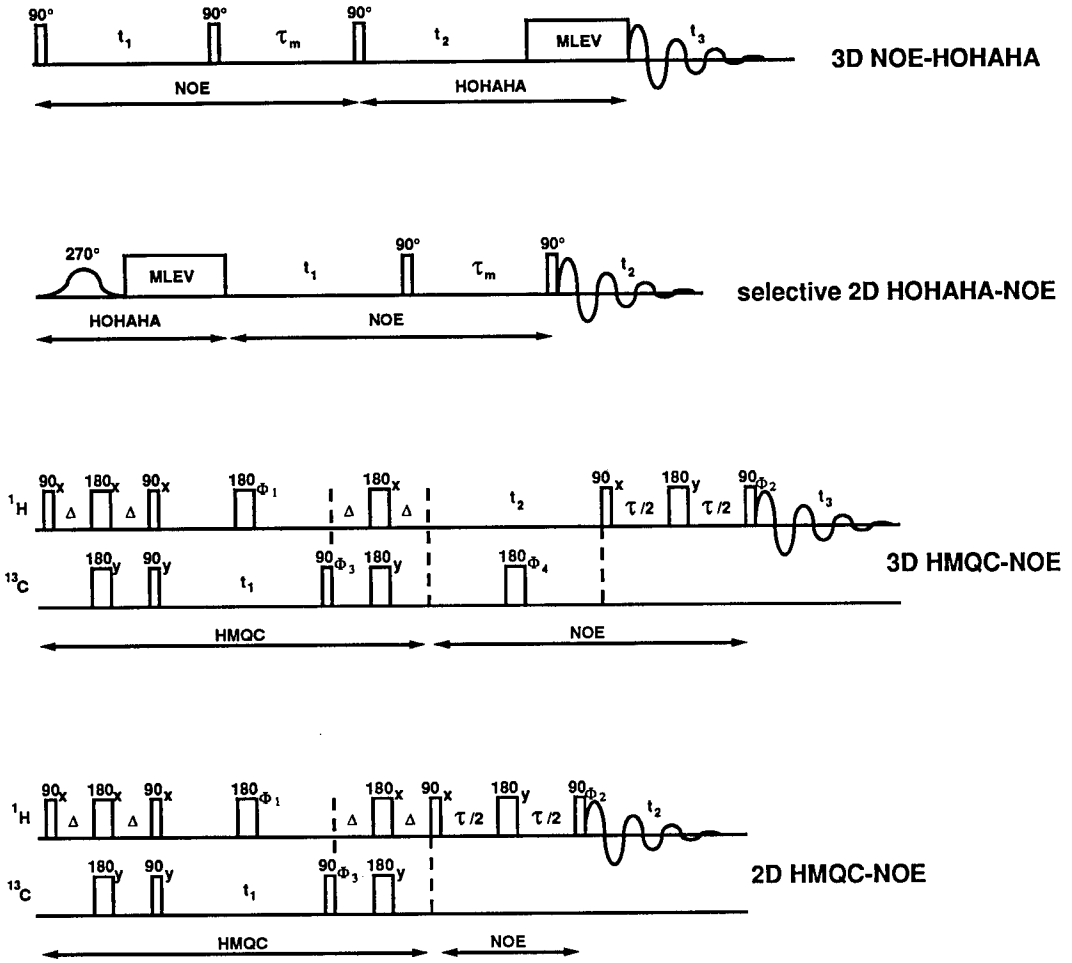

Fig. 1. Pulse sequences of 2D and 3D NOE-HOHAHA and 2D and 3D HMQC-NOE experiments. For the 3D NOE-HOHAHA experiment a phase cycle of 4 steps was used on the pulse after the NOE mixing period. Combined with a phase cycle of two steps for axial peak suppression this yielded 8 scans for each FID. Acquisition was preceded by 2 dummy scans. Positive and negative frequencies in ω_1 and ω_2 were separated by independent TPPI on the preparation pulse and the pulse prior to the t_2 evolution period. For the selective 2D HOHAHA-NOE experiment quadrature detection was combined with a phase cycle of 4 steps for the pulse after t_1. Together with inversion of the phase for the MLEV-17 mixing sequence and axial peak suppression this resulted in a 64-steps phase cycle. Positive and negative frequencies in ω_1 were separated by TPPI on the pulses after t_1 and the receiver. The following phase cycling is used for 2D and 3D HMQC-NOE: $\Phi_1 = 2(x,x,-x,-x,y,y,-y,-y)$; $\Phi_2 = 8(x),8(-x)$; $\Phi_3 = 8(x,-x)$; $\Phi_4 = 4(x,-x,-x,x)$; acq $= 2(x,-x),4(-x,x),2(x,-x)$. Positive and negative frequencies in ω_1 were separated by independent TPPI on the 90° ^{13}C pulse before t_1. For the 3D experiment positive and negative frequencies in ω_2 were separated by independent TPPI on all pulses prior to the t_2 evolution period.

HOHAHA line, the diagonal of the cross section, which is equivalent to a column in a 2D HOHAHA experiment. The NOE part of the sequence affords a NOE cross peak between GlcNAc-1 H-4 and GlcNAc-2 H-1 on a horizontal (ω_2) line starting from the GlcNAc-1 H-4 signal on the HO-

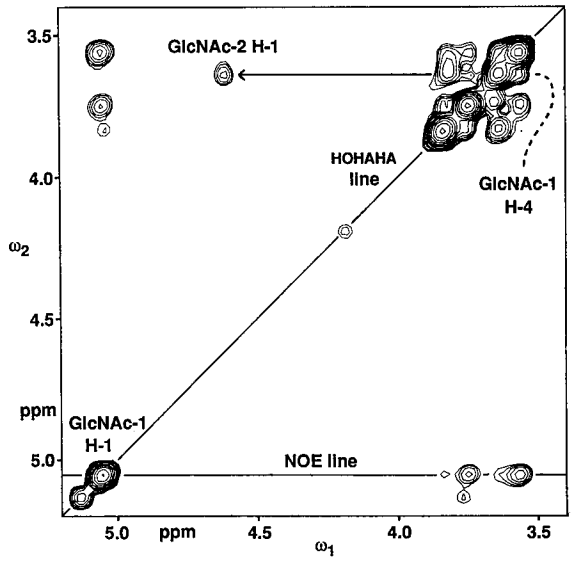

Fig. 2. Cross sections perpendicular to the ω_3 axis at the frequency of GlcNAc-1 H-1 of the 3D NOE-HOHAHA spectrum of a 20-mM solution of **1**.

HAHA line. This NOE can be observed due to magnetization transfer via the HOHAHA isotropic mixing to the GlcNAc-1 proton.

NOEs on a single ω_2 line in an ω_3 cross section suffer to the same extent from magnetization losses during the HOHAHA transfer. A direct comparison of NOEs with reference NOEs on a single ω_2 line is therefore possible.

The question arises if it is sensible to measure these cross sections directly as 2D spectra. To obtain the ω_3 cross section of GlcNAc-5/5′ H-1 at $\delta = 4.59$ ppm (Fig. 3A) as a 2D spectrum it is necessary to give a selective pulse on GlcNAc-5/5′ H-1, directly followed by the HOHAHA mixing period. The subspectra of the GlcNAc-5/5′ residues are selected as in 1D HOHAHA (Davis and Bax, 1985). The 1D HOHAHA sequence now serves as preparation period for a 2D NOE experiment. In the selective 2D HOHAHA-NOE spectrum (for the pulse sequence see Fig. 1) magnetization that is not transferred during the NOE mixing period is found on the diagonal and the NOEs on horizontal lines (Fig. 3B). This spectrum is very similar to the ω_3 cross section of the 3D spectrum of **1** (Fig. 3A). The short measuring time of the selective 2D experiment compared to that of the 3D experiment leads to a lower signal-to-noise ratio. However, the important NOEs between GlcNAc-5/5′ H-4 and Gal-6/6′ H-1 can be observed in both spectra. Not only the lower signal-to-noise ratio, but also t_1-noise ridges and magnetization loss due to the applied selective pulse are responsible for the lower quality of the 2D spectrum. On the other hand the 2D alternative yields a better digital resolution and can be used to acquire build-up series in order to give more reliable estimates of proton-proton distances. Since in nonselective 3D NMR all measuring time is used for excitation of the whole spectrum, resulting in a high signal-to-noise ratio, it is recommended to record 3D spectra instead of a series of selective 2D HOHAHA-NOE spectra.

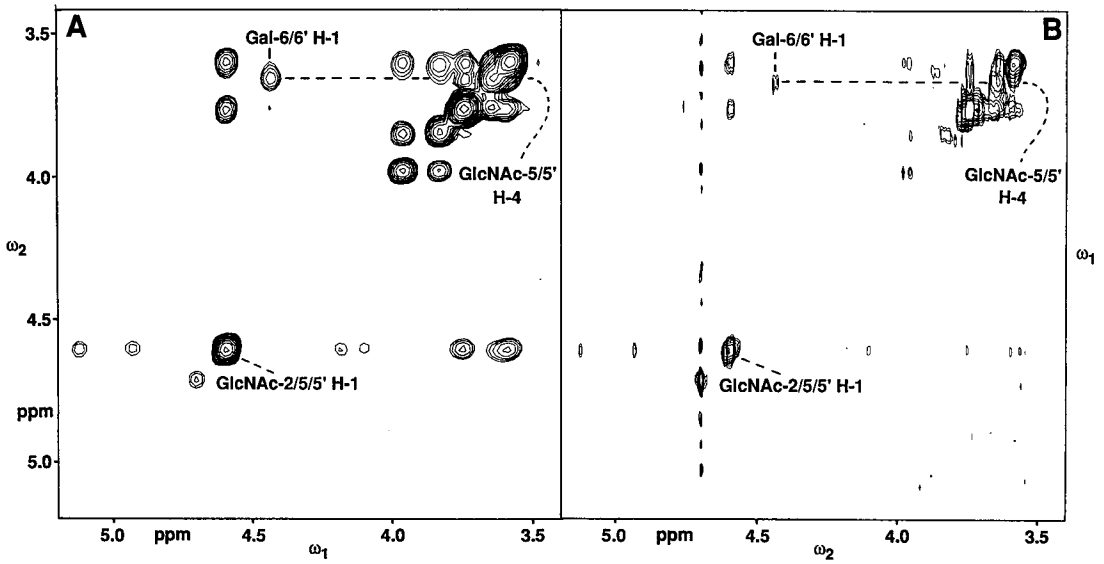

Fig. 3. An ω_3 cross section at the frequency of GlcNAc-5/5' H-1 of the 3D NOE-HOHAHA spectrum of **1** (A) compared to a selective 2D HOHAHA-NOE spectrum of a 20-mM solution of **1** (B).

Heteronuclear 2D and 3D experiments

To detect NOEs of protons which cannot be measured due to spectral overlap or poor HOHAHA transfer the resolution of a 2D NOE spectrum can be enhanced by adding the ^{13}C frequency domain as the third dimension, leading to the 3D HMQC-NOE experiment (Fig. 1) (Fesik and Zuiderweg, 1988; De Waard et al., 1990). For the interpretation of these spectra ω_1 cross sections are used, which contain the NOEs of protons attached to the ^{13}C atoms, resonating at the ω_1 frequency of that cross section. The NOEs of a proton are found on a single line perpendicular to the ω_2 axis. This line is comparable with a row in a 2D NOE spectrum as is shown for GlcNAc-5/5' H-1 and for Man-4 H-1 of **1** (Fig. 4). The NOE magnetization transfer takes place after the labeling of the protons with a ^{13}C frequency in the HMQC part. When measuring at natural abundance, NOEs have to be expected on protons attached to ^{12}C. Therefore, no ^1H-^{13}C coupling is present on the NOE cross peaks. The magnetization which is not transferred during the NOE part and is referred to as HMQC cross peaks, is found on the diagonal of an ω_1 cross section ($\omega_2 = \omega_3$). These cross peaks are split by the ^1H-^{13}C coupling (Fig. 4).

If only one proton is attached to a carbon atom the ω_1 cross section of a 3D HMQC-NOE experiment contains only one NOE line. This observation combined with the low resolution in the ^{13}C domain leads to the conclusion that the extra ^1H dimension mainly serves as a compensation for the low ^{13}C resolution. Since carbohydrates contain many tertiary carbon atoms, which have a good ^{13}C chemical shift dispersion, the 3D HMQC-NOE experiment is not optimal. For these reasons the 2D analogue of 3D HMQC-NOE, which has a considerably higher ^{13}C resolution, is regarded to be a worthwhile alternative. However, the use of the 2D HMQC-NOE experiment does not allow the stereospecific assignment of NOEs to protons of methylene or methyl groups as well as the assignment of NOEs to protons attached to carbon atoms which still have overlap-

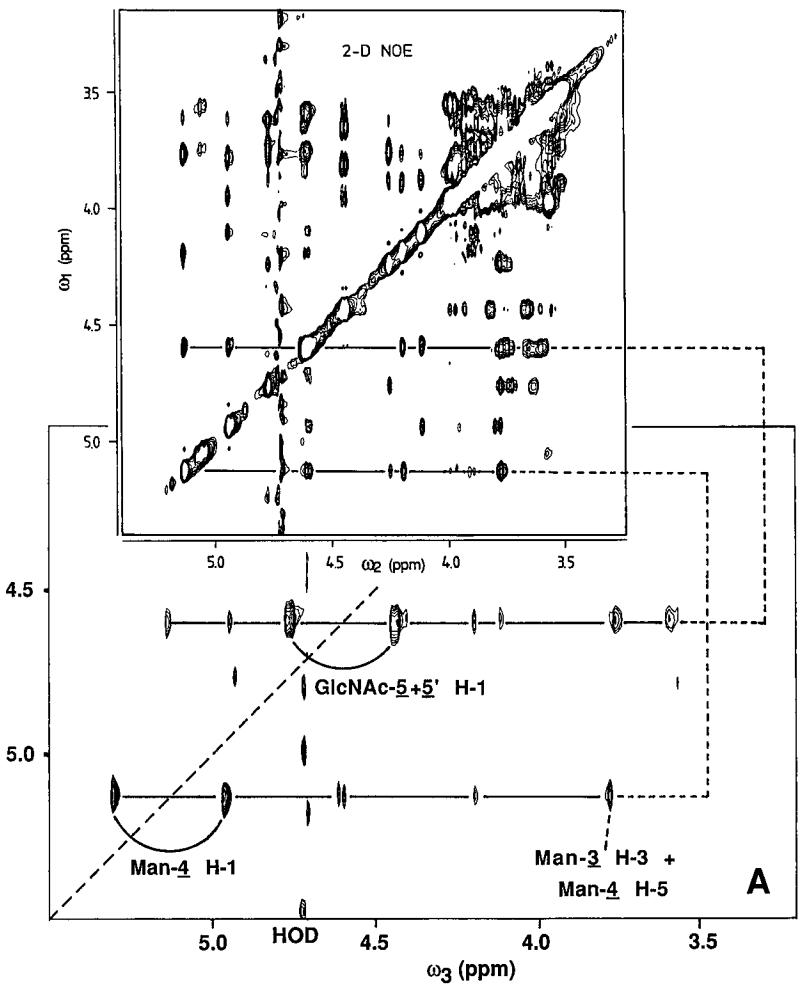

Fig. 4. Cross section perpendicular to the ω_1 axis at $\delta = 101$ ppm of the 3D HMQC-NOE spectrum of a 20-mM solution of **1**. The insert shows a conventional 2D NOE spectrum of **1**.

ping resonances. Nevertheless a preference exists to record 2D HMQC-NOE spectra for carbohydrates instead of the 3D originals.

The effect of ^{13}C decoupling during the acquisition is shown for a part of the bulk region of the corresponding 2D HMQC-NOE spectrum (Fig. 5). The doubling of the HMQC cross peaks due to the ^{1}H-^{13}C coupling results in more overlap (Fig. 5A). For example the NOE between NeuAc H-5 and H-4 is hidden under the HMQC cross peak, while in the spectrum of the decoupled experiment this NOE is discernible (Fig. 5B). Although the experiment without decoupling contains some extra overlap, it offers the unique possibility to identify NOEs between protons having identical chemical shifts (Wagner, 1989). This is demonstrated by the NOE between NeuAc H-9/9′ and H-8. In Fig. 5B this NOE is hidden under the HMQC cross peak of NeuAc H-9, resonating at almost the same chemical shift as the H-8, whereas in Fig. 5A this NOE is not disturbed by

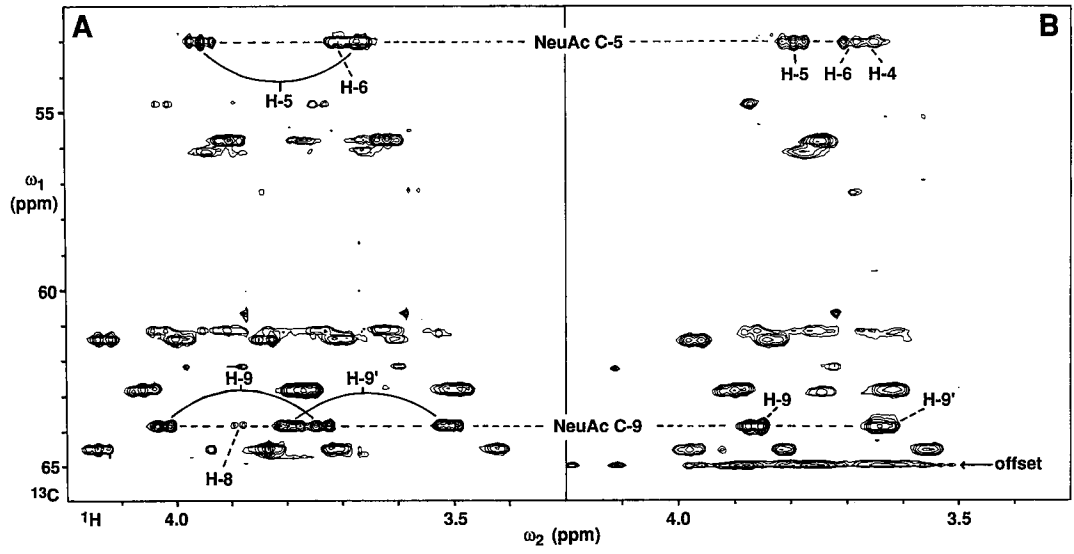

Fig. 5. Part of the bulk region of coupled (A) and decoupled (B) 2D HMQC-NOE spectra of a 60-mM solution of **2**. Heating of the sample due to decoupling during the acquisition causes some artefacts, for example at the offset frequency as indicated in (B).

overlap. These examples show that both versions of HMQC-NOE, decoupled and nondecoupled, provide complementary information in cases of overlap of NOEs with the HMQC cross peaks.

CONFORMATION OF THE DIANTENNARY OLIGOSACCHARIDE

For conformational analysis it is important that the intensities of the NOEs can be measured reliably. For this reason the NOEs of the experiments described here are evaluated by comparison with those obtained from a 2D NOE experiment. Proton-proton distances were calculated from these NOEs (cf. Experimental Section) and are summarized in Table 1. The 2D NOE spectrum is recorded under the same conditions as the homo- and heteronuclear 3D experiments, with the same NOE mixing time. The NOEs between GlcNAc-5 H-1 and Man-4 H-1 and H-2, and similarly between GlcNAc-5′ H-1 and Man-4′ H-1 and H-2, have been chosen for comparison. Distances have been calculated using the intraresidue NOEs between Man-4 H-1 and H-2 as a reference. The distance between Man-4 H-2 and H-3 has been calculated from the intraresidue NOE between these atoms as an additional check. In ω_3 cross sections of the 3D NOE-HOHAHA spectrum these NOEs are found on the NOE lines as indicated in Fig. 6. Moreover, they can also be identified as 3D cross peaks. For example, the NOE-plane NOEs of Man-4 H-1 (Fig. 6A) can also be found as 3D NOEs in the ω_3 cross section of Man-4 H-2 (Fig. 6B). For these 3D NOEs magnetization is transferred during HOHAHA mixing to H-2. It is important to note, however, that all 3D cross peaks on a HOHAHA line suffer from the *same* magnetization loss during isotropic mixing. This allows calibrating distances for interresidual NOEs if a cross peak involving an intraresidual NOE is present on the same HOHAHA line.

TABLE 1
PROTON-PROTON DISTANCES CALCULATED FROM NOEs IN 2D AND 3D HOMONUCLEAR AND HETERONUCLEAR EXPERIMENTS[a]

NOE	Calculated proton-proton distances (Å)						
	20 mg **1**					60 mg **2**	
	2D NOE	3D NOE-HOHAHA		3D HMQC-NOE	2D HMQC-NOE	2D HMQC-NOE	
		2D cross peak	3D cross peak		coupled	coupled	decoupled
Man-4 H-1 / GlcNAc-5 H-1	2.5	2.4	2.4	2.3	2.5	2.5	n.d.[b]
Man-4′ H-1 / GlcNAc-5′ H-1	2.6	2.4	2.3	2.2	2.8	2.4	2.7
Man-4 H-2 / GlcNAc-5 H-1	2.7	2.5	2.6	2.5	2.5	2.5	2.2
Man-4′ H-2 / GlcNAc-5′ H-1	2.7	2.4	2.7	2.5	2.5	2.2	2.1
Man-4 H-2 / Man-4 H-3	2.8	2.5	2.7	2.2	2.2	2.3	2.3
Man-4′ H-2 / Man-4′ H-3	2.6	2.4	2.7	2.2	2.2	2.3	2.0

[a] NOEs between Man-4/4′ H-1 and H-2 served as references.
[b] Not detectable due to overlap with the HMQC cross peak of GlcNAc 5/5′.

The distances derived from the 2D and 3D NOE-HOHAHA and HMQC-NOE experiments are in reasonable agreement with those of the conventional 2D NOE experiment. In Table 2 the interresidue NOEs assigned in the 2D and 3D homonuclear and heteronuclear spectra are summarized together with the distances calculated from these NOEs. Since the experimental distances do not necessarily correspond to a single conformation, the weighted averaging of an ensemble of possible conformations may give better results (Cumming and Carver, 1987a). This approach which takes the whole shape of the energy well into account rather than only the energy minima, seems attractive from a theoretical point of view. However, in this work (Cumming and Carver, 1987b) HSEA calculations were used, which are known to narrow the shape of the energy wells due to exaggerated steric interactions. It has been demonstrated that relaxation of all internal coordinates of the constituent monosaccharides through an extensive molecular mechanics scheme will allow more conformational states to be reached (Breg et al., 1989). Therefore, the ensemble average approach is expected to give reliable results only when the energy profile has been accurately determined. Since accurate energy profiles are not known, a simplified method of averaging which considers only the energy minima will be used here. This averaging method contains the implicit assumption that the energy wells around these minima have the same shape.

Starting from a database of conformations for disaccharide fragments belonging to *N*-glycans (Imberty et al., 1990a), the proton-proton distances over glycosidic linkages are calculated for each minimal-energy conformation. From these distances a weighted average is calculated using the energy levels of each conformation (Imberty et al., 1990a). In the following section glycosidic linkages of the diantennary compound will be discussed separately.

The GlcNAc-2 β(1-4)GlcNAc-1 linkage

The interresidue NOE between GlcNAc-2 H-1 and GlcNAc-1 H-4 could only be measured in

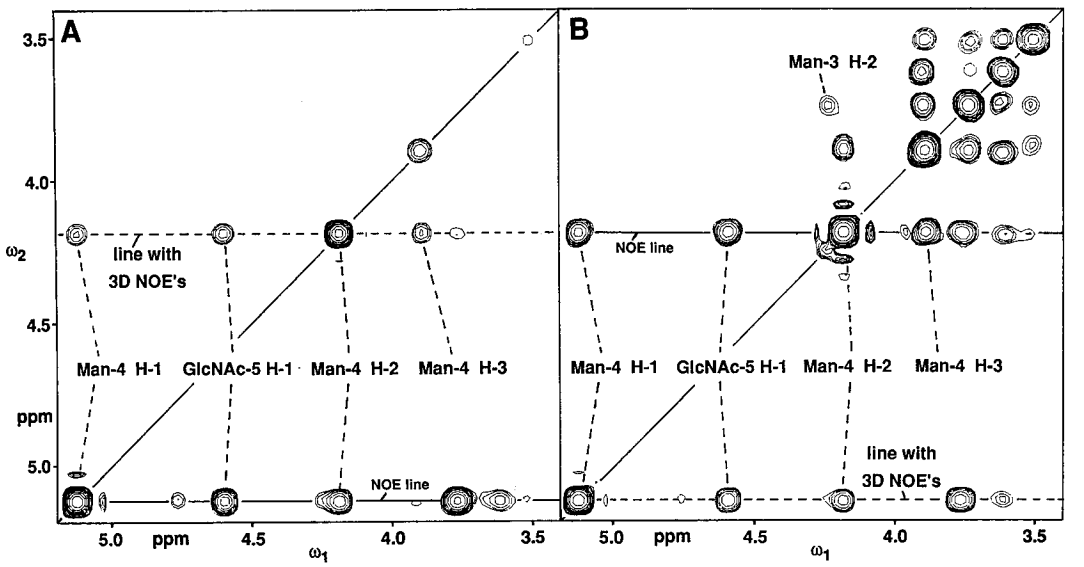

Fig. 6. Cross sections perpendicular to the ω_3 axis at the frequency of Man-4 H-1 (A) and at the frequency of Man-4 H-2 (B) of the 3D NOE-HOHAHA spectrum of a 20-mM solution of **1**.

TABLE 2
PROTON-PROTON DISTANCES CALCULATED FROM INTERRESIDUE NOEs

NOE	Experiment	Observed at	Intraresidue reference NOE and distance (Å)		Experimental interresidue distance (Å)	Literature values	Weighted averaged distance
GlcNAc-2 H-1/ GlcNAc-1 H-4	3D NOE-HOHAHA	GlcNAc-1 H-1	GlcNAc-1 H-2/H-4	2.7	3.0	2.4[c]	2.3
Man-3 H-1/ GlcNAc-2 H-4	2D NOE		Man-3 H-1/H-2	2.5	2.3	2.4[c]	2.3
	3D HMQC-NOE	Man-3 C-1	Man-3 H-1/H-2	2.5	2.2		
	2D HMQC-NOE-2[b]	Man-3 C-1	Man-3 H-1/H-2	2.5	2.4		
Man-4 H-1/ Man-3 H-3	3D HMQC-NOE	Man-3 C-3	Man-3 H-2/H-3	2.5	2.3	2.1[d]	2.3
	2D HMQC-NOE-1[b]	Man-3 C-3	Man-3 H-2/H-3	2.5	2.3		
	2D HMQC-NOE-2[b]	Man-3 C-3	Man-3 H-2/H-3	2.5	2.3		
	2D HMQC-NOE-3[b]	Man-3 C-3	Man-3 H-2/H-3	2.5	2.3		
Man-4 H-1/ Man-3 H-2	3D NOE-HOHAHA	Man-4 H-1	Man-4 H-1/H-2	2.6	3.1	3.1[d]	2.6
	3D NOE-HOHAHA	Man-3 H-2	Man-3 H-1/H-2	2.5	2.8		
	2D HMQC-NOE-2[b]	Man-4 C-1	Man-4 H-1/H-2	2.6	3.0		
	2D HMQC-NOE-2[b]	Man-3 C-2	Man-3 H-1/H-2	2.5	3.3		
	2D NOE		Man-4 H-1/H-2	2.6	2.8		
	2D NOE		Man-3 H-1/H-2	2.5	3.0		
Man-4 H-5/ Man-3 H-2	3D NOE-HOHAHA	Man-4 H-2	Man-4 H-3/H-5	2.6	3.0	2.5[e]	2.8
	3D NOE-HOHAHA	Man-4 H-2	Man-4 H-4/H-5	3.1	3.0		
	2D HMQC-NOE-1[b]	Man-4 C-5	Man-4 H-4/H-5	3.1	3.8		
	2D HMQC-NOE-2[b]	Man-4 C-5	Man-4 H-4/H-5	3.1	3.6		
Man-4′ H-3/ Man-3 H-4	3D NOE-HOHAHA	Man-4′ H-2	Man-4′ H-2/H-3	2.4	3.2	–	3.2
	3D NOE-HOHAHA	Man-4′ H-2	Man-4′ H-3/H-4	3.1	3.3		
	3D NOE-HOHAHA	Man-4′ H-2	Man-4′ H-3/H-5	2.6	3.6		
Man-4′ H-5/ Man-3 H-4	3D NOE-HOHAHA	Man-4′ H-2	Man-4′ H-3/H-5	2.6	4.4	–	2.7
	3D NOE-HOHAHA	Man-4′ H-2	Man-4′ H-4/H-5	3.1	4.0		
Gal-6/6′ H-1/ GlcNAc-5/5′ H-4	3D NOE-HOHAHA	GlcNAc-5/5′ H-1	GlcNAc-5/5′ H-2/H-4	2.7	2.8	–	–
	2D HOHAHA-NOE		GlcNAc-5/5′ H-2/H-4	2.7	3.0		
	3D HMQC-NOE	GlcNAc-5/5′ C-4	GlcNAc-5/5′ H-4/H-5	3.0	3.3		
	2D HMQC-NOE-1[b]	GlcNAc-5/5′ C-4	GlcNAc-5/5′ H-4/H-5	3.0	3.3		
	2D HMQC-NOE-2[b]	GlcNAc-5/5′ C-4	GlcNAc-5/5′ H-4/H-5	3.0	3.2		
	2D HMQC-NOE-3[b]	GlcNAc-5/5′ C-4	GlcNAc-5/5′ H-4/H-5	3.0	3.0		

[a] Tabulated are the reference NOEs together with the reference distances. Some literature values, and weighted averaged distances derived from a database of 3D structures of disaccharides (Imberty et al., 1990) are given. For the 3D NOE-

the 3D NOE-HOHAHA spectrum (see Fig. 3 and Vuister et al., 1989). In the HMQC-NOE experiments this NOE is below the noise level. A distance of 2.4 Å was found for the corresponding atoms in the glycopeptide Manα(1-6)[Xylβ(1-2)]Manβ(1-4)GlcNAcβ(1-4)[Fucα(1-3)]GlcNAcβ(1-*N*)Asn-Glu-Ser-Ser (Bouwstra et al., 1990), being in agreement with the weighted average value. However, the distance calculated from the 3D NOE-HOHAHA spectrum (3.0 Å) is not in accordance with this value. There are 3 possible explanations for this difference: (i) The energy levels of the various conformations of the GlcNAcβ(1-4)GlcNAc linkage are different for the diantennary structure due to backfolding of the Manα(1-6) branch. In the lowest energy conformation of the disaccharide, with $(\varphi_H,\psi_H) = (35, 15)$ (Imberty et al., 1990a), the distance between GlcNAc-2 H-1 and GlcNAc-1 H-4 is 2.2 Å. The experimental distance of 3.0 Å (Table 2) would imply a considerably larger contribution from the conformations with $(\varphi_H,\psi_H) = (25, 175)$ and $(\varphi_H,\psi_H) = (70, -150)$ (Imberty et al., 1990a), since for these conformations a distance of 3.5 Å has been calculated. (ii) The experimental value is not estimated reliably due to overlap of the reference NOE cross peak with other cross peaks. If the reference NOE intensity is taken too high, the interresidue proton-proton distance will be too large. In several instances this kind of overlap within the bulk region will be unavoidable in 3D NOE-HOHAHA spectroscopy, since the resolution of these spectra is low. (iii) The possible influence of the different peptide parts.

The Man-3 β(1-4)GlcNAc-2 linkage

The 3 lowest energy conformations for the Manβ(1-4)GlcNAc disaccharide (Imberty et al., 1990a) show for each conformation similar distances between the Man-3 H-1 and GlcNAc-2 H-4 atoms. Therefore, changes in population distributions of these conformations will have negligible effects on the weighted average distance, and the experimental distances (Table 2) derived from 2D NOE and HMQC-NOE experiments are in agreement with the weighted average distance. In 3D NOE-HOHAHA this NOE could not be quantified, due to the low resolution of the spectrum causing overlap with other NOEs.

The Man-4 α(1-3)Man-3 linkage

For this linkage two different conformations have been suggested. For the conformation with $(\varphi_H,\psi_H) = (-50, -20)$ a NOE is observable between the Man-4 H-5 and Man-3 H-2 atoms (Brisson and Carver, 1983a,b). The presence of this NOE was confirmed in a study on a synthetic partially deuterated trimannoside (Cumming et al., 1986). This NOE can be assigned unambiguously in 3D NOE-HOHAHA (see Fig. 6B and Vuister et al., 1989) and in the HMQC-NOE experiments. The NOE observable between Man-4 H-1 and Man-3 H-2 atoms is consistent with the other conformation with $(\varphi_H,\psi_H) = (-35, 55)$. This NOE cannot be ascribed to spin-diffusion

---

HOHAHA is indicated which ω_3 cross section, for the 3D HMQC-NOE experiment which ω_1 cross section, and for the 2D HMQC-NOE experiments which row is used for observation of a NOE.

[b] 2D HMQC-NOE-1, -2, and -3, are short-hand notations for the nondecoupled 2D HMQC-NOE experiment of the 20-mM sample of **1**, the nondecoupled experiment of the 60-mM sample of **2**, and the decoupled experiment of the 60-mM sample of **2**, respectively.

[c] Values derived from Bouwstra et al., 1990.

[d] Values derived from Homans et al., 1986.

[e] Value derived from Brisson and Carver, 1983.

[f] Conformations for this linkage not yet available in database.

effects (Homans et al., 1987a). Since both NOEs are present in the spectra described here, it is reasonable to assume that in accordance with the recently suggested higher degree of flexibility for the Manα(1-3)Man linkage (Imberty et al., 1990b) at least both conformations occur. Energy calculations (Imberty et al., 1990a) show 3 main energy minima for this linkage. In Table 2 the experimental distances calculated from the observed NOEs are compared to the weighted averages calculated from the energy minimal conformations. The distance between the Man-4 H-1 and Man-3 H-3 atoms is almost the same for the 3 conformations with lowest energy. The values derived from 2D and 3D HMQC-NOE are in agreement with the weighted average distance. The distance between the Man-4 H-5 and Man-3 H-2 atoms as calculated from the 3D NOE-HOHAHA experiment, differs 0.2 Å from the weighted average distance. The NOE between Man-4 H-5 and Man-3 H-2 is only of qualitative importance due to uncertainty in the reference NOE cross peak. The experimental values for the distance between Man-4 H-1 and Man-3 H-2 are approximately 3 Å, in agreement with literature data (Homans et al., 1987a). These values are higher than the weighted average distance of 2.6 Å.

The Man-4′ α(1-6)Man-3 linkage

Two NOEs between Man-3 H-4 and Man-4′ H-3 and H-5 atoms, which are in the bulk region and are of comparable intensity, could be identified in the 3D NOE-HOHAHA spectrum (Vuister et al., 1989). In both HMQC-NOE experiments these NOEs are below the noise level. The occurrence of both NOEs is only compatible with the GG-conformation, with $\omega_H = 180°$. Since the Man-4′ H-2 is not coinciding with other signals, the intraresidue NOE between H-2 and H-3 can serve as a reliable reference for estimation of the distance between Man-4′ H-3 and Man-3 H-4. The experimental distance of 3.2 Å derived in this way (Table 2) is in excellent agreement with the weighted average distance of 3.2 Å. For calculation of the distance between Man-4′ H-5 and Man-3 H-4 only NOEs in the bulk region (Man-4′ H-3/H-4 and H-3/H-5) are available as references. They should be interpreted with care, since NOEs in the bulk region may overlap with other NOEs. The results show a discrepancy between the experimental and the weighted average distances between Man-4′ H-5 and Man-3 H-4. It is likely that this discrepancy is caused by overlap of the reference NOEs, because the calculated distance between Man-3 H-4 and Man-4′ H-5 is much larger than that between Man-3 H-4 and Man-4′ H-3 although the NOE intensities between Man-4′ H-3 and H-5 and Man-3 H-4 are of the same order of magnitude.

So far, for complex diantennary structures averaging between the GG and GT conformers has been suggested (Brisson and Carver, 1983c; Homans et al., 1986). Both NMR spectroscopy and computational techniques (HSEA-type and MM2 calculations) have been used to evaluate the rotational population distribution for the (1-6) linkage. Depending on the technique and the method of data analysis, the results show either a preference for the GG conformation (Berman, 1987) or a preference for the GT conformation (Paulsen et al., 1987; Cumming and Carver, 1987b) or somewhere in between (Brisson and Carver, 1983c; Homans et al., 1986; Carver and Cumming, 1987). The GG/GT ratio according to the energy minima used here is 3:1, which accounts for the two observed intraresidue NOEs.

The GlcNAcβ(1-2)Man linkage

The data on this linkage are in agreement with 1D and 2D NOE data and with NOEs calculated from an ensemble average relaxation matrix (Cumming and Carver, 1987a).

The Galβ(1-4)GlcNAc linkage

The NOE between GlcNAc-5 H-4 and Gal-6 H-1 coinciding with that between GlcNAc-5′ H-4 and Gal-6′ H-1 is observable in the homo- and heteronuclear experiments. For the evaluation of the experimental data no conformations for this linkage are available in the databank for disaccharide structures (Imberty et al., 1990a).

The NeuAcα(2-6)Gal linkage

In the experiments described here no NOEs are identified between NeuAc and Gal. The conformation of this linkage has been studied in a model compound (Breg et al., 1989; Sabesan et al., 1991). HSEA calculations revealed a number of possible low-energy conformations. Although for each of these conformations some NOEs are expected, none of these could be measured.

Finally, the HMQC-NOE experiments provide the possibility of measuring the NOEs between the protons of the glycerol side chain of sialic acid (De Waard et al., 1990). These NOEs, which can be found in the bulk region, are only measurable in HMQC-NOE experiments, since these protons cannot be reached with the HOHAHA part of the homonuclear sequences, due to the small coupling between H-6 and H-7 in sialic acid. The strong NOE cross peaks between H-6 and H-7 and the low-intensity NOEs between H-7 and H-8 are consistent with the conformation of the glycerol side chain as suggested by measurements of $^3J_{H,H}$ coupling constants by Christian et al. (1987) and with a crystal structure determination (Kooijman et al., 1990).

CONCLUSIONS

The present work illustrates the usefulness of homo- and heteronuclear 3D NMR techniques for the assignment of NMR spectra of complex oligosaccharides as well as for the study of their spatial structure. 3D NOE-HOHAHA experiments allow detection of NOEs of protons resonating in the bulk region by magnetization transfer through scalar couplings to nonoverlapping protons. The long measuring time of a 3D NOE-HOHAHA spectrum, needed to record sufficient increments in the ω_1 and ω_2 frequency domains, affords a high signal-to-noise ratio. As an alternative, selective 2D HOHAHA-NOE spectroscopy provides the possibility of measuring NOE build-up series and could result in higher digital resolution compared to the 3D spectrum, however, at the expense of a much lower signal-to-noise ratio. Therefore, the 3D NOE-HOHAHA experiments are preferred in most cases.

In the heteronuclear experiments the resolution of the carbon spectrum is used to separate the proton signals in the bulk region. The low signal-to-noise ratio of the heteronuclear experiments measured at natural abundance is a disadvantage, but spectral editing with the carbon frequency as ω_1 domain affords the possibility of gaining supplementary information, not available in homonuclear experiments. Since the extra proton dimension in the 3D HMQC-NOE experiment is only rarely needed and since the resolution in the ^{13}C domain is low in the 3D experiment, the 2D version of this experiment appears to be adequate in most cases.

The information on NOEs derived from the experiments described here is not only of qualitative, but also of quantitative value. As shown in Table 2, in most cases the NOE-derived distances match those based on the weighted average calculated low-energy conformations.

The application of homonuclear 3D NMR and heteronuclear 2D and 3D NMR experiments reveals distance information, which is not obtainable from homonuclear 2D NOE spectra.

EXPERIMENTAL SECTION

Homonuclear 2D and 3D NMR experiments

The phase-sensitive 3D NOE-HOHAHA spectrum of a 20-mM sample of **1** was recorded at 500 MHz on a Bruker AM500 spectrometer at 304 K and pH 7.0. The pulse sequence is depicted in Fig. 1. During the relaxation delay of 0.45 s the HDO resonance was suppressed by irradiation. The NOE mixing time was 350 ms. Isotropic mixing was induced by an MLEV-17 (Bax and Davis, 1985) sequence of 94 ms with trim pulses at the beginning and at the end. Acquisition was preceded by 2 dummy scans. FIDs of 8 scans were recorded with a size of 1K. This was repeated independently for 144 incremental t_1 and 144 incremental t_2 values, resulting in a total measuring time of approximately 63 h. Positive and negative frequencies in ω_1 and ω_2 were separated by independent TPPI on the preparation pulse and the pulse prior to the t_2 evolution period. Spectral width in all 3 frequency domains was 2272.7 Hz. Data were zero-filled twice in the t_1 and t_2 domains before Fourier transformation. Shifted sine-square windows were used in all 3 time domains. The resulting dataset of 256 × 256 × 512 points was baseline-corrected in all frequency domains by a third-order polynomial fit.

The selective 2D HOHAHA-NOE spectrum of a 20-mM sample of **1** was recorded under the same conditions as the 3D spectrum (see Fig. 1). A selective Gaussian pulse of 154 ms (270°) (Emsley and Bodenhausen, 1989) was applied on the GlcNAc-5/5′ H-1. The HOHAHA and NOE mixing times were the same as for the 3D experiment; 400 FIDs of 2048 data points were recorded, with 32 scans per t_1 value, preceded by 4 dummy scans. The time-domain data were multiplied with a shifted sine-square window. After Fourier transformation the resulting dataset of 1024 × 1024 points was baseline-corrected in both frequency domains by a third-order polynomial fit.

Heteronuclear 2D and 3D NMR experiments

The phase-sensitive 3D HMQC-NOE spectrum of a 20-mM sample of **1** was recorded at 500 MHz on a Bruker AM500 spectrometer at 304 K and pH 7 using the pulse sequence shown in Fig. 1. The relaxation delay was 0.6 s, Δ was 1.78 ms, and the NOE mixing time was 350 ms. Acquisition was preceded by 4 dummy scans. FIDs of 16 scans were recorded with a size of 1K. This was repeated independently for 112 incremental t_1 and 96 t_2 values, resulting in a total measuring time of approximately 63 h. Positive and negative frequencies in ω_1 and ω_2 were separated by independent TPPI on the 90° ^{13}C pulse for ω_1 and on all pulses prior to the t_2 evolution period for ω_2. The spectral width in the ^{1}H frequency domains was 2272.7 Hz, and in the ^{13}C frequency domain 11 364 Hz. Data were zero-filled twice in the t_2 and t_1 domains before Fourier transformation. A shifted sine-square window multiplication was used in the t_3 domain, while a Hamming window was used in the t_2 and t_1 domains (Ernst et al., 1987). The resulting data set of 256 × 256 × 512 points was baseline-corrected in all frequency domains by a third-order polynomial fit.

The 2D HMQC-NOE spectra were recorded under the same conditions as the 3D spectrum with the pulse sequence shown in Fig. 1. For all spectra the delay Δ was 1.78 ms, and the NOE mixing time was 350 ms. For the spectrum of the 20-mM sample of **1** the relaxation delay was 1.0 s. Acquisition was preceded by 4 dummy scans, and 2048 t_1 increments of 48 scans each were recorded with a size of 2K, resulting in a total measuring time of approximately 60 h. For recording of the spectrum of a 60-mM sample of **2** the relaxation delay was 0.7 s. Acquisition was preceded

by 4 dummy scans, and 2048 t_1 increments of 64 scans each were recorded with a size of 2K, resulting in a total measuring time of approximately 66 h. For the ^{13}C-decoupled spectrum of a 60-mM sample of **2** the relaxation delay was 1.2 s. Acquisition was preceded by 4 dummy scans, and 2048 t_1 increments of 48 scans each were recorded with a size of 2K, resulting in a total measuring time of approximately 66 h. For decoupling during the acquisition a GARP sequence (Shaka et al., 1985) was applied through a modified Bruker BSV-3 amplifier. For all spectra, the spectral width in the ^1H frequency domain was 2272.7 Hz and in the ^{13}C frequency domain 11 364 Hz. Shifted sine-square multiplications were used in the t_2 and t_1 domains. The data sets of 1024 × 1024 points resulting after Fourier transformation were baseline-corrected in both frequency domains by a third-order polynomial fit.

Calculation of experimental distances

NOE cross peaks were integrated in two dimensions. For the 3D NOE-HOHAHA experiments ω_3 or ω_2 cross sections, and for the 3D HMQC-NOE experiment ω_1 cross sections were used for integration. The ratio between an interresidue NOE and a reference NOE remains the same in adjacent cross sections. For this reason integration in 3 dimensions is not necessary. Interresidue proton-proton distances are calculated by relating their NOE cross-peak intensities to those of intraresidue proton-proton pairs at known distances by the equation

$$r_{ij} = r_0(a_0/a_{ij})^{1/6}$$

where r_{ij} = distance to be determined, r_0 = known distance, a_{ij} = cross-peak intensity of a pair of protons at an unknown distance and a_0 = cross-peak intensity of a pair of protons at a known distance.

Calculation of weighted average distances

For each minimum-energy conformation of a linkage provided by the database of conformations for disaccharide fragments in *N*-glycans (Imberty et al., 1990a) interresidue distances were calculated on an Evans & Sutherland PS300 graphic display station connected to a local VAX cluster. Weighted average distances were calculated by the equation

$$r_w = [1/\Sigma\{(1/r_i)^6 * f(i)\}]^{1/6}$$

where f(i) = a normalized Boltzmann factor: $f(i) = \exp\{-E_i/RT\}/\Sigma\exp\{-E_j/RT\}$, r_w = weighted average distance, r_i = distance of conformation i and E_i = energy level of conformation i.

ACKNOWLEDGEMENTS

This work was supported by the Netherlands Foundation for Chemical Research (SON) with financial aid of the Netherlands Foundation of Scientific Research (NWO) and by the Netherlands Program for Innovation Oriented Carbohydrate Research (IOP-k) with financial aid from the Ministry of Economic Affairs and the Ministry of Agriculture, Nature management and Fisheries. Thanks are due to Profs. G. Spik and J. Montreuil, Université des Sciences et Techniques de Lille Flandres Artois, France, for the gift of the diantennary compound **1**, and to Dr. G.J. Gerwig for preparation of the diantennary compound **2**.

REFERENCES

Bax, A. and Davis, D.G. (1985) *J. Magn. Reson.*, **65**, 355–360.

Berman, E. (1987) *Eur. J. Biochem.*, **165**, 385–391.

Bouwstra, J.B., Spoelstra, E.C., De Waard, P., Leeflang, B., Kamerling, J.P. and Vliegenthart, J.F.G. (1990) *Eur. J. Biochem.*, **190**, 113–122.

Breg, J., Kroon-Batenburg, L.M.J., Strecker, G., Montreuil, J. and Vliegenthart, J.F.G. (1989) *Eur. J. Biochem.*, **178**, 727–739.

Brisson, J.-R. and Carver, J.P. (1983a) *Biochemistry*, **22**, 1362–1368.

Brisson, J.-R. and Carver, J.P. (1983b) *Biochemistry*, **22**, 3671–3680.

Brisson, J.-R. and Carver, J.P. (1983c) *Biochemistry*, **22**, 3680–3686.

Bush, C.A. (1989) *Bull. Magn. Reson.*, **10**, 73–95.

Carver, J.P. and Cumming, D.A. (1987) *Pure Appl. Chem.*, **11**, 1465–1476.

Carver, J.P., Michnick, S.W., Imberty, A. and Cumming, D.A. (1989) *CIBA Foundation Symposium 145 (Carbohydrate Recognition in Cellular Function)* Wiley & Sons, Chichester, pp. 6–25.

Christian, R., Schulz, G., Brandstetter, H.H. and Zbiral, E. (1987) *Carbohydr. Res.*, **162**, 1–11.

Cumming, D.A. and Carver, J.P. (1987a) *Biochemistry*, **26**, 6664–6676.

Cumming, D.A. and Carver, J.P. (1987b) *Biochemistry*, **26**, 6676–6683.

Cumming, D.A., Dime, D.S., Grey, A.A., Krepinsky, J.J. and Carver, J.P. (1986) *J. Biol. Chem.*, **261**, 3208–3213.

Dabrowski, J. (1989) *Meth. Enzymol.*, **176**, 122–156.

Davis, D.G. and Bax, A. (1985) *J. Am. Chem. Soc.*, **107**, 7197–7198.

De Waard, P., Boelens, R., Vuister, G.W. and Vliegenthart, J.F.G. (1990) *J. Am. Chem. Soc.*, **112**, 3232–3234.

Emsley, L. and Bodenhausen, G. (1989) *J. Magn. Reson.*, **82**, 211–221.

Ernst, R.R., Bodenhausen, G. and Wokaun, A. (1987) *Principles of Nuclear Magnetic Resonance in One and Two Dimensions*, Clarendon Press, Oxford, p. 103.

Fesik, S.W. and Zuiderweg, E.R.P. (1988) *J. Magn. Reson.*, **78**, 588–593.

Homans, S.W. (1990) *Progr. NMR Spectrosc.*, **22**, 55–81.

Homans, S.W., Dwek, R.A., Boyd, J., Mahmoudian, M., Richards, W.G. and Rademacher, T.W. (1986) *Biochemistry*, **25**, 6342–6350.

Homans, S.W., Dwek, R.A. and Rademacher, T.W. (1987) *Biochemistry*, **26**, 6553–6560.

Imberty, A., Gerber, S., Tran, V. and Pérez, S. (1990a) *Glycoconj. J.*, **7**, 27–54.

Imberty, A., Tran, V. and Pérez, S. (1990b) *J. Comput. Chem.*, **11**, 205–216.

Inagaki, F., Kodama, C., Suzuki, M. and Suzuki, A. (1987) *FEBS Lett.*, **219**, 45–50.

Kooijman, H., Kroon-Batenburg, L.M.J., Kroon, J., Breg, J.N and De Boer, J.L. (1990) *Acta Crystallogr. C*, **46**, 407–410.

Paulsen, H., Peters, T. and Sinnwell, V. (1987) *Carbohydr. Res.*, **165**, 251–266.

Sabesan, S., Bock, K. and Paulson, J.C. (1991) *Carbohydr. Res.*, **218**, 27–54.

Shaka, A.J., Barker, P.B. and Freeman, R. (1985) *J. Magn. Reson.*, **64**, 547–552.

Tvaroska, I., Pérez, S. and Marchessault, R.H. (1978) *Carbohydr. Res.*, **61**, 97–106.

Vliegenthart, J.F.G., Dorland, L. and Van Halbeek, H. (1983) *Adv. Carbohydr. Chem. Biochem.*, **41**, 209–374.

Vuister, G.W., De Waard, P., Boelens, R., Vliegenthart, J.F.G. and Kaptein, R. (1989) *J. Am. Chem. Soc.*, **111**, 772–774.

Wagner, G. (1989) *Meth. Enzymol.*, **176**, 93–113.